FEBS Letters 586 (2012) 3582–3589

journal homepage: www.FEBSLetters.org

Structural insights into the calcium-dependent interaction between calbindin-D28K and caspase-3

Benjamin G. Bobay [a,1], Amanda L. Stewart [a,1,2], Ashley T. Tucker [a], Richele J. Thompson [a], Kristen M. Varney [b], John Cavanagh [a,*]

[a] Department of Molecular and Structural Biochemistry, North Carolina State University, 128 Polk Hall, Raleigh, NC 27695, United States
[b] Department of Biochemistry and Molecular Biology, University of Maryland School of Medicine, 108 N. Greene St., Baltimore, MD 21201, United States

ARTICLE INFO

Article history:
Received 27 July 2012
Revised 27 August 2012
Accepted 30 August 2012
Available online 13 September 2012

Edited by Gianni Cesareni

Keywords:
Calbindin-D28K
Caspase-3
Isothermal titration calorimetry
Molecular docking

ABSTRACT

The regulation of apoptosis involves a complicated cascade requiring numerous protein interactions including the pro-apoptotic executioner protein caspase-3 and the anti-apoptotic calcium-binding protein calbindin-D28K. Using isothermal titration calorimetry, we show that calbindin-D28K binds caspase-3 in a Ca^{2+}-dependent fashion. Molecular docking and conformational sampling studies of the Ca^{2+}-loaded capase-3/calbindin-D28K interaction were performed in order to isolate potentially crucial intermolecular contacts. Residues in the active site loops of caspase-3 and EF-hands 1 and 2 of calbindin-D28K were shown to be critical to the interaction. Based on these studies, a model is proposed to help understand how calbindin-D28K may deactivate caspase-3 upon binding.

Structured summary of protein interactions:
Calbindin-D28K and Caspase-3 bind by isothermal titration calorimetry (View interaction)

1. Introduction

The life and death of cells must be balanced if tissue homeostasis is to be maintained – there should neither be too much growth nor too little death [1]. Normal cells accommodate this balance by invoking apoptosis. Apoptosis is triggered via two main signaling pathways [2]. The *intrinsic pathway* initiates from within the cell by developmental cues or as a result of severe cell stress (e.g., DNA damage). The *extrinsic pathway* initiates when a pro-apoptotic ligand binds to pro-apoptotic receptors on the cell surface. Cross-talk between these pathways occurs at the level of the effector/executioner caspase proteins (caspases-3, -6 and -7). Once activated, these intracellular enzymes destroy proteins that are essential for cell survival and trigger cell death. A third pathway, the *granzyme B pathway*, is initiated by the constituents of cytotoxic granules that are released upon encounter with transformed or virally infected target cells [3]. Caspases-3, -7, -8 and -10 are directly processed by granzyme B whereas caspases-2, -6 and -9 are processed in a second, caspase-3-dependent, wave of processing. All three signaling pathways route through caspase-3.

Caspase-3 targets the peptide sequence Asp-Glu-Val-Asp (DEVD) with cleavage occurring on the C-terminal side of the second aspartic acid residue [4,5]. The catalytic action of caspase-3 is mediated by the sulfhydryl group of Cys 163 and the imidazole ring of His 121 (PDB:1CP3). These are referred to as the catalytic residues. His 121 stabilizes the carbonyl group of the key aspartate residue, while Cys 163 attacks to cleave the peptide bond. Cys 163 and Gly 122 also stabilize the tetrahedral transition state of the substrate–enzyme complex [5]. If caspase-3 function is impeded then apoptosis is hindered. Not surprisingly, therapeutics are being developed to affect various caspase family members. With few exceptions, all of the proof-of-concept preclinical studies with caspase inhibitors have been performed with active-site mimetic peptide ketones. From a drug development standpoint, the most attention has been paid to caspase-3 [6]. However, to this point no therapeutics have reached the clinic, making alternate approaches for inhibiting caspase-3 action appealing.

The Ca^{2+}-binding EF-hand protein calbindin-D28K is known to interact with caspase-3 and inhibit apoptosis. Its anti-apoptotic properties have been demonstrated in neuronal cells, osteocytes, osteoblasts, and lymphocytes [7–9]. It is suggested that calbindin-D28K is not a substrate for caspase-3 itself (i.e., does not occupy the caspase-3 binding site) as it is not cleaved significantly by the enzyme [9]. When apoptosis is initiated, Ca^{2+} concentrations

* Corresponding author. Address: Department of Molecular and Structural Biochemistry, North Carolina State University, 128 Polk Hall, Box 7622, Raleigh, NC 27695-7622, United States. Fax: +1 919 515 2047.
E-mail address: john_cavanagh@ncsu.edu (J. Cavanagh).
[1] These authors contributed equally to this work.
[2] Present address: Department of Chemistry, University of North Florida, 1 UNF Drive, Jacksonville, FL 32224, United States.

0014-5793/$36.00
http://dx.doi.org/10.1016/j.febslet.2012.08.032

within the cell increase and a decrease in apoptosis is observed [9]. Calbindin-D28K also inhibits degradation of synthetic and natural caspase-3 substrates while other Ca^{2+}-binding proteins do not. This indicates that its ability to limit apoptosis is not simply due to Ca^{2+}-buffering properties, but also because it directly interacts with caspase-3. The caspase-3/calbindin-D28K interaction has been shown to be specific since other Ca^{2+}-binding proteins (calmodulin, S100, calbindin-D9k and osteocalcin) do not inhibit caspase-3. Binding between calbindin-D28K and caspase-3 has been suggested to be independent of Ca^{2+}, i.e., the binding event is the same regardless of whether calbindin-D28K is in its apo-state or in one of its partially/fully Ca^{2+}-loaded forms [9].

Our previous studies indicate a notable difference between the structures of apo-calbindin-D28K and its fully-loaded ($4Ca^{2+}$) form [10]. It would be surprising if these two forms of calbindin-D28K bound to caspase-3 identically. Consequently, we wanted to further examine any Ca^{2+}-dependency of the caspase-3/calbindin-D28K interaction. To do this we used a combination of circular dichroism, NMR and isothermal titration calorimetry. Our studies reveal that the caspase-3/calbindin-D28K interaction is, in fact, dependent upon calbindin-D28K's level of Ca^{2+}-loading. Additionally, we performed computational docking studies and conformational sampling simulations, using the structures of fully Ca^{2+}-loaded calbindin-D28K (NMR) and caspase-3 (X-ray). These studies furnish the first model for the complex and suggest a possible mechanism by which calbindin-D28K contributes to the deactivation of caspase-3 and inhibits apoptosis.

2. Materials and methods

2.1. Sample preparation

The expression and purification of calbindin-D28K have been described [10–12]. Apo-calbindin-D28K solutions were prepared with 5 mm EDTA in all purification steps. The expression and purification of caspase-3 is as previously described [13].

2.2. Circular dichroism

All CD measurements were obtained on an Applied Photophysics Chirascan Plus CD Spectrometer with calbindin-D28K samples at 5 μM for far UV (260–190 nm) measurements at 25 °C. The samples were equilibrated overnight in 10 mM Tris buffer (pH 6.5), with appropriate $CaCl_2$ concentrations to obtain 1:1, 1:2, 1:3, and 1:4 calbindin-D28K/Ca^{2+} molar ratios. Apo-calbindin-D28K samples were equilibrated overnight in 10 mM Tris (pH 6.5), 5 mM EDTA.

2.3. Isothermal titration calorimetry

For ITC measurements, purified calbindin-D28K and caspase-3 were buffer exchanged into 50 mM HEPES (pH 7.5), 100 mM NaCl, 1 mM β-mercaptoethanol (βME) and 10% glycerol. For the apo-samples, 1 mM EDTA was added. For the fully and partially Ca^{2+}-loaded states of calbindin-D28K, equivalent molar ratios of $CaCl_2$ were added from 1 to 6 (to ensure complete loading). The experiments were performed at 26 °C using an AutoITC200 microcalorimeter (GE MicroCal Inc.). The apo- and partially Ca^{2+}-loaded experiments were performed by injecting 2 μl of 800 μM calbindin-D28K into a 200 μl sample cell containing 50 μM caspase-3. The fully Ca^{2+}-loaded experiments were performed by injecting 2 μl of 500 μM calbindin-D28K into a 200 μl sample cell containing 30 μM caspase-3. A total of 20 injections were performed with a spacing of 180 s and a reference power of 7 μcal/s. Control experiments for each buffer (apo- and Ca^{2+}-loaded states) were also performed, and heat of dilution was measured by titrating calbindin-D28K into buffer alone. The heat of dilution generated by calbindin-D28K was subtracted, and the binding isotherms were fit to a one-site and two-site binding model using Origin 7 Software (MicroCal, Inc.). The data analysis protocol and appropriate equations for analyzing the caspase-3/calbindin-D28K interaction by ITC are provided in Supplementary data.

2.4. 'Blind' molecular docking

High ambiguity driven protein–protein docking (HADDOCK) was set up as follows: coordinate files for Ca^{2+}-loaded calbindin-D28K and caspase-3 were obtained from the PDB (2G9B and 1CP3, respectively) [12,14,15]. All residues with solvent accessibility of 50% or greater were defined as 'active'. No residues in either protein were defined as being 'passive'. The caspase-3 PDB was modified to include only one monomer of caspase-3 and the dimerization interface of caspase-3 was excluded as a region for interaction between calbindin-D28K and caspase-3. Default HADDOCK parameters were used. Final structures were grouped using a minimum cluster-size of 4 with a Cα RMSD <7.5 Å using ProFit (http://www.bioinf.org.uk/software/profit/) and further grouped based on the "HADDOCK SCORE".

2.5. 'Targeted' molecular docking

The 'targeted' molecular docking was performed similarly, with the following exceptions: (1) active residues (3, 9, 22, 25–27, 34, 41, 45, 48–51, 53, 56, 59–60, 63–64, 67, 69–70, 83, 86–87) for calbindin-D28k were defined as residues within EF-hands 1 and 2 with greater than 50% solvent accessibility; (2) passive residues (97–98, 105, 109, 112- 113, 121, 128, 132, 135, 137, 140–141, 157–159, 174–175, 183, 185, 189, 192–193, 196–197, 200–201, 204, 209, 220–221, 224, 228–229, 236, 244, 250, 261) for calbindin-D28K were defined as residues not within EF-hands 1 and 2 with greater than 50% solvent accessibility; (3) active residues (53–54, 56–58, 60, 62–63, 68, 209–210, 246, 248, 250, 252–255) for caspase-3 were defined as residues with greater than 50% solvent accessibility on the active site surface (including the loop-bundles); and (4) passive residues (35, 38, 42, 72, 80, 82, 89, 94, 102, 105, 107, 110, 123–124, 135, 137, 138, 147, 149, 153, 166–167, 170, 173, 185, 224–225, 228–229, 277) for caspase-3 were defined as residues not within the active site surface with greater than 50% solvent accessibility.

2.6. Refinement of the docked solutions

The lowest energy structure from the 'targeted' molecular docking within the highest populated cluster of structures was refined with 2000 ps of implicit solvent refinement implemented in AMBER 11 [16] to account for solvent effects and eliminate structural imperfections as defined via WHATCHECK [17]. The structure was further analyzed by PROCHECK [18] to confirm stereochemical quality and also to check for clashes in the interface region by tleap in AMBER; no significant clashes were detected.

2.7. Conformational sampling simulation

Conformational transitions simulations were performed on the caspase-3 structure using tCONCOORD [19]. Standard tCONCOORD parameters were used; maximum distance for hydrogen bonds was set to 2.6 Å with a minimum angle for hydrogen bonds of 140° [19]. Hydrophobic backbone–backbone, sidechain–backbone and sidechain–sidechain protections were used throughout the simulation. Bond flexibility was set to 0.04 Å, angle flexibility was set to 0.1 Å and 9.0°, planarity tolerance was set to 0.03, flexibility for restricted dihedrals was set to 0.1%, and flexibility for

non-restricted dihedrals was set to 0.6%. The same tCONCOORD procedure was used for all PDBs.

3. Results

3.1. Circular dichroism

Previous NMR studies showed that calbindin-D28K transitions from an ordered, structured conformation in its apo-state through a set of more disordered states when loaded with successive amounts of Ca^{2+} [10]. When it is finally fully Ca^{2+}-loaded ($4Ca^{2+}$), it adopts a *different* ordered, structured conformation. These CD data were obtained for apo-calbindin-D28K and calbindin-D28K loaded with $1Ca^{2+}$, $2Ca^{2+}$, $3Ca^{2+}$ and $4Ca^{2+}$. All spectra display minima at 208 and 222 nm, which is characteristic of alpha-helical proteins. Supplementary Fig. 1 shows an overlay of CD data from each calbindin-D28K Ca^{2+}-loaded state. Interestingly, the extent of helical content appears constant in all states. Accordingly, we

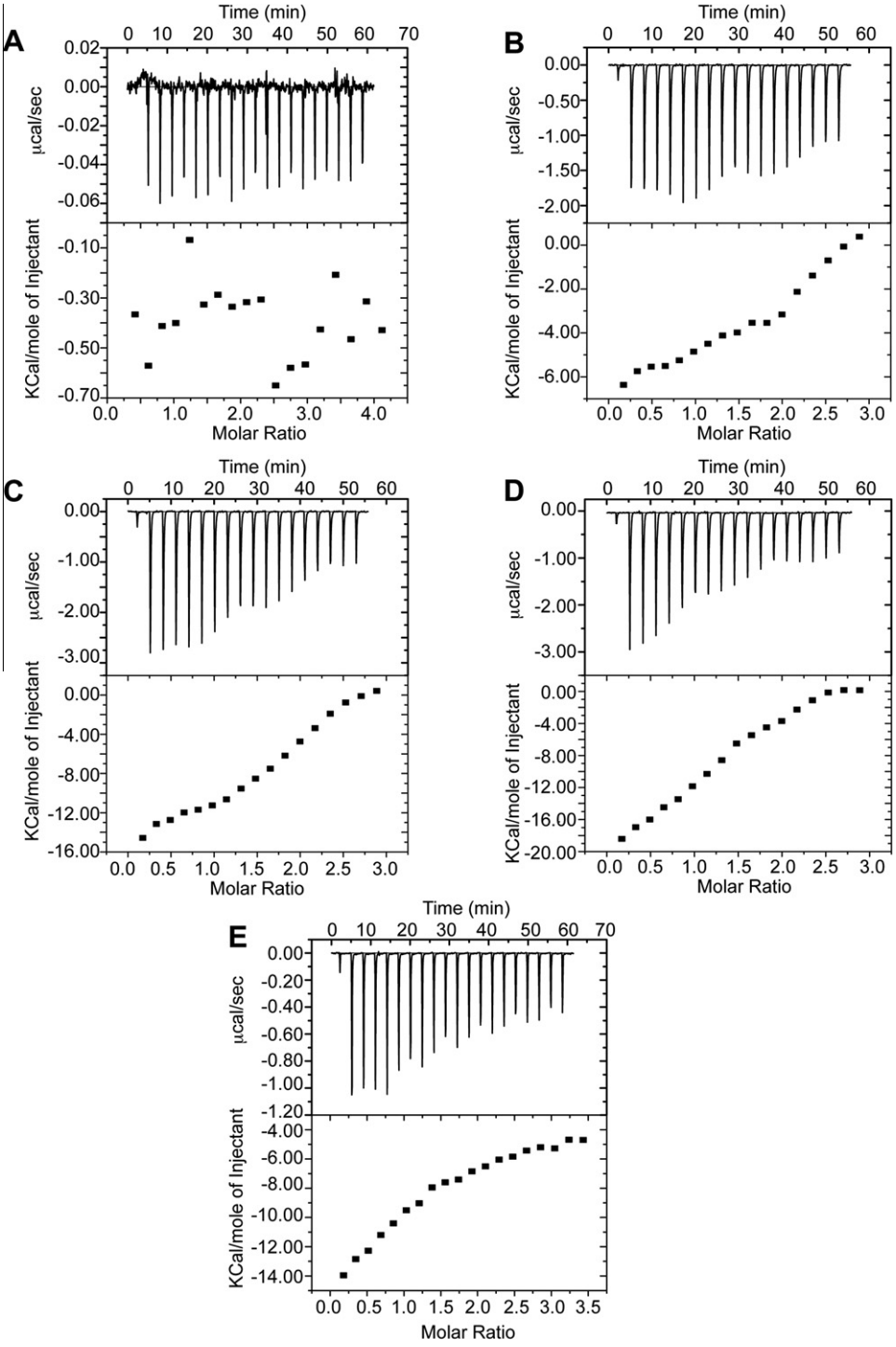

Fig. 1. ITC raw data and binding curve for the interaction between calbindin-D28K and caspase-3. (A) Interaction between apo calbindin-D28K and caspase-3. (B) ITC interaction between 1:1 calbindin-D28K/Ca^{2+} and caspase-3. (C) ITC interaction between 1:2 calbindin-D28K/Ca^{2+} and caspase-3. (D) ITC interaction between 1:3 calbindin-D28K/Ca^{2+} and caspase-3. (E) ITC interaction between fully Ca^{2+}-loaded calbindin-D28K and caspase-3.

investigated how different Ca^{2+}-loaded states of calbindin-D28K bound to caspase-3 using ITC. All samples were checked for structural quality prior to ITC analysis by CD and NMR.

3.2. Isothermal titration calorimetry

ITC binding experiments (Fig. 1) indicate the following: (i) apo-calbindin-D28K does not bind caspase-3; (ii) $1Ca^{2+}$-loaded calbindin-D28K binds to caspase-3 with the binding most closely approximating a two-site model with an N-value (reaction stoichiometry) of 0.64 and 1.32; (iii) $2Ca^{2+}$-loaded calbindin-D28K binds to caspase-3 with the binding most closely approximating a two-site model (N-values of 1.28 and 1.90); (iv) $3Ca^{2+}$-loaded calbindin-D28K binds to caspase-3 with the binding moving from a two-site model more towards a one-site model (N-values of 1.60 and 0.53); (v) fully Ca^{2+}-loaded calbindin-D28K binds to caspase-3 with the binding most closely approximating a one-site model (N-value of 1.05). In each case the binding occurs with low micromolar affinity. These data are summarized in Table 1.

3.3. Computational docking

Initially, 'blind' molecular docking of calbindin-D28K to caspase-3 was performed. Here, the only contact restraint invoked was that interacting residues should have a minimum of 50% solvent accessibility. The 'blind' molecular modeling resulted in 13 clusters shown in Supplementary Fig. 2. These structural clusters suggested that the main location for the interaction occurs at the active site loops of caspase-3 with EF-hands 1 and 2 of calbindin-D28K. The 'active site loops' consist of loops 1, 3 and 4 from one monomeric unit of the caspase-3 dimer and loop 2' from the other monomeric unit [20]. In each case, calbindin-D28K does not directly interact with the catalytic residues His 121 and Cys 163 of caspase-3. We define 'not directly interacting' as a distance (Cα–Cα) of at least 4.5 Å between residues in calbindin-D28K and the catalytic residues in caspase-3. Lending support to these preliminary studies was that the binding region identified on calbindin-D28K is similar to a region on calbindin-D28K shown previously to be involved in interactions with peptides derived from known targets [11].

The results of the blind docking laid the groundwork for a more directed approach that involved targeting solvent accessible residues within EF-hands 1 and 2 of calbindin-D28K with the active site loops of caspase-3. This resulted in 3 total clusters with cluster-1 containing ~70% of the docked solutions. Here, a cluster-is defined as a minimum of 20 structures (10% of the total structures solved) and a maximum RMSD of 7.5 Å over all structures (Supplementary Fig. 3). The lowest energy structure within the greatest populated cluster-was further refined in AMBER (Fig. 2). Fig. 2A shows the caspase-3 dimer binding symmetrically to two calbindin-D28K molecules. Fig. 2B shows the interaction more clearly, with only one caspase-3 monomer and one calbindin-D28K depicted. Since cluster-1 is by far the most populated, we focus our mechanistic discussions on this model, though other lesser populated clusters may have some relevance.

Table 1
Isothermal titration calorimetry data for the interaction between caspase-3 and calbindin-D28K.

Calbindin/Ca^{2+} molar ratio	K_d 1, μM (error)	K_d 2, μM (error)	N1 (error)	N2 (error)	Binding mode
Apo protein	No binding				
1:1	0.86(0.80)	0.28(0.24)	0.64(0.69)	1.32(0.25)	Two-site
1:2	2.35(0.89)	1.03(0.82)	1.28(1.21)	1.90(0.20)	Two-site
1:3	1.41(2.25)	0.12(0.15)	1.60(0.33)	0.53(0.46)	Two-site
1:4	7.12(0.94)	–	1.05(0.04)	–	One-site

[a]Standard deviations shown in parentheses. Stoichiometry is included for each sample as N1 and N2.

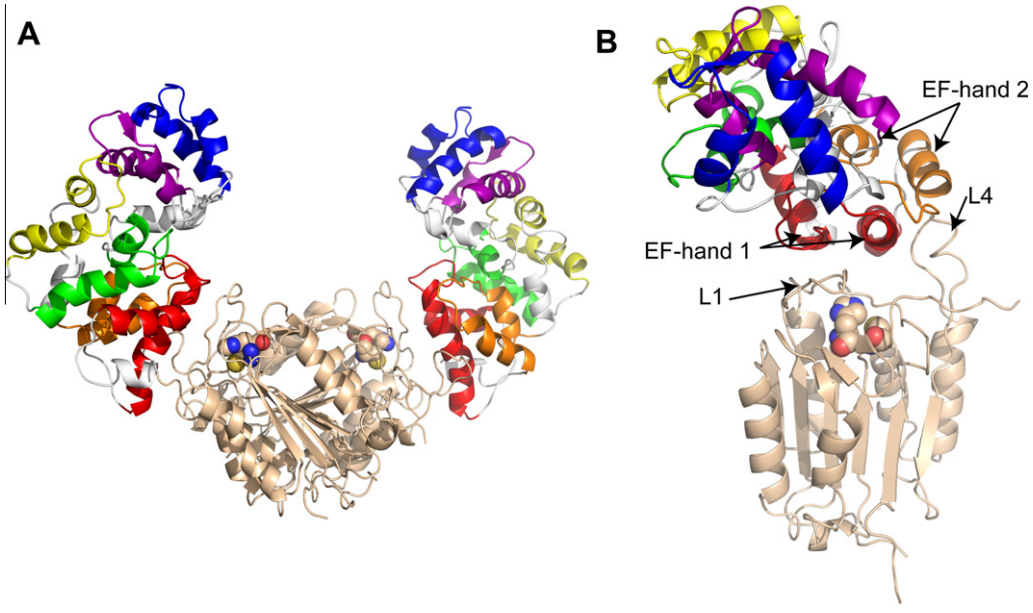

Fig. 2. Lowest energy AMBER refined complex. (A) The lowest energy AMBER refined complex between calbindin-D28K and caspase-3. Caspase-3 is colored beige while calbindin-D28K is colored with regard to its EF-hand pairs: EF-hand 1 (red), EF-hand 2 (orange), EF-hand 3 (yellow), EF-hand 4 (green), EF-hand 5 (blue) and EF-hand 6 (purple). All other α-helical domains connecting the EF-hands are colored white. (B) Wild-type caspase-3/calbindin-D28K complex. Coloring is the same as in panel (A). Caspase-3 catalytic residues are shown as spheres with hydrogens removed. Loops and EF-hands are labeled for clarity.

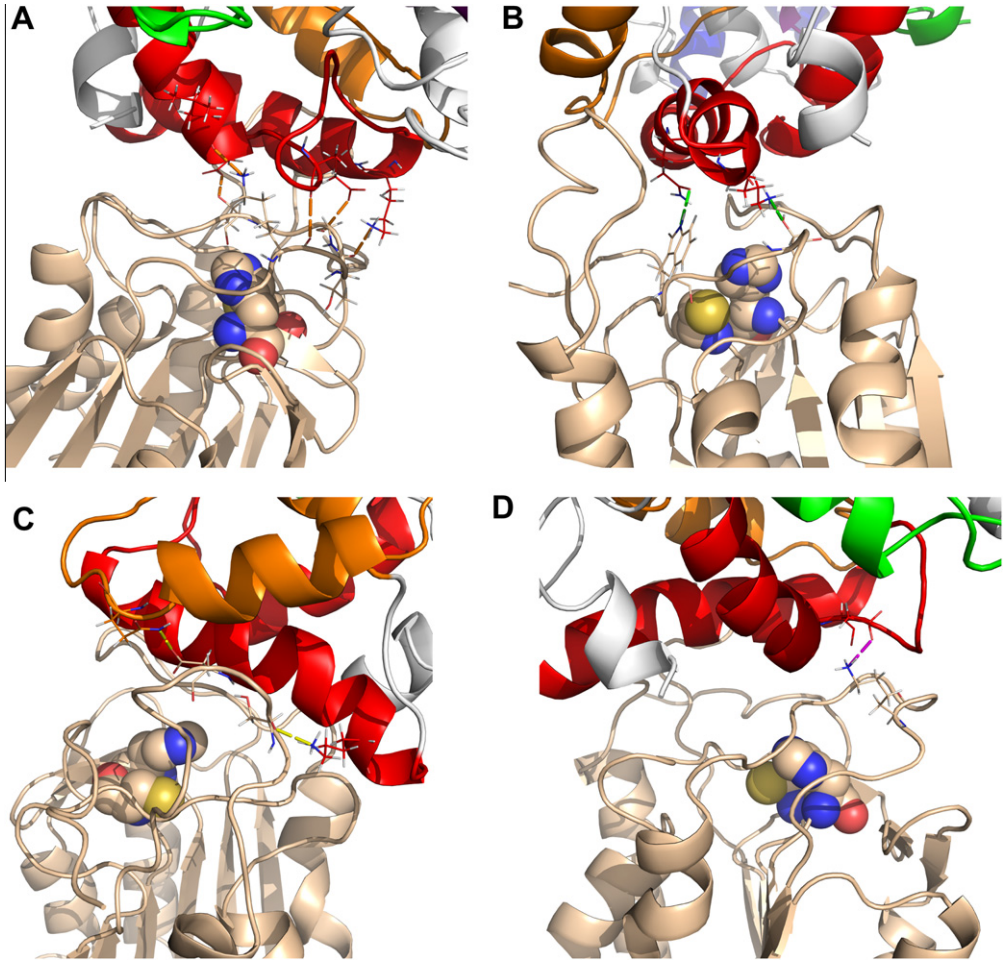

Fig. 3. Hydrogen bond and salt bridge interactions. Coloring is identical to Fig. 2. (A) Hydrogen bonds (orange lines) between calbindin-D28K and caspase-3's loop 1. (B) Hydrogen bonds (green lines) between calbindin-D28K and caspase-3's loop 3. (C) Hydrogen bonds (yellow lines) between calbindin-D28K and caspase-3's loop 4. (D) Salt bridge (magenta line) between calbindin-D28K and caspase-3's loop 1. Caspase-3 catalytic residues are shown as spheres with hydrogens removed.

As discussed below, the main interaction region consists of EF-hands 1 and 2 from calbindin-D28K with the active site loops of caspase-3, particularly loop 1 – though all loops contribute to some degree. This region is dominated by protein/protein interactions between residues 21–27 of calbindin-D28K (end of α-helix 1 of EF-hand 1) and residues 57–65 of caspase-3 (loop 1). The helical domain of EF-hand 1 (α-helix 2–residues 33–50) governs the interaction by intercalating itself between loops 1 and 2 with interactions to caspase-3 residues 59–62 (loop 1), 166 (loop 2), 206–211 (loop 3) and 250–256 (loop 4). The helical domain of EF-hand 2 (α-helix 1–residues 56–67) primarily interacts with caspase-3 residues 251–255 (loop 4). Also, potentially stabilizing the interaction between calbindin-D28K and caspase-3 are a network of hydrogen bonds. These interactions are predominantly located between EF-hand 1 (α-helices 1 and 2) of calbindin-D28K and loop 1 of caspase-3 (Fig. 3A – orange lines). Additionally several more hydrogen bonds are suggested to be present between: (a) EF-hand 1 (α-helix 2) of calbindin-D28K and loop 3 of caspase-3 (Fig. 3B – green lines), (b) EF-hand 1 (α-helix 2) and EF-hand 2 (α-helix 1) of calbindin-D28K and loop 4 of caspase-3 (Fig. 3C – yellow lines). Finally, there is an important salt bridge between Asp 24 of calbindin-D28K and Lys 57 of caspase-3 (Fig. 3D – magenta line).

When comparing the structures of caspase-3 in its unbound form (X-ray) and its bound form (docked model) it is evident that loops 1 and 4 show the biggest change in position (see Section 4).

3.4. Conformational sampling

Since loops 1 and 4 of caspase-3 showed the largest conformational adjustment on calbindin-D28K binding, we performed conformational sampling simulations on these loops to investigate any potential motional changes due to the interaction. As discussed below, in the case of both loops there is a notable reduction in the conformational space being sampled upon calbindin-D28K binding. Comparing loop RMSD's between uncomplexed and complexed states there is a 22% decrease for loop 1 and a 15% decrease for loop 4. These data suggest that the conformational shifts of caspase-3 loops 1 and 4 upon binding calbindin-D28K are accompanied by a reduction in flexibility in both cases, trapping them in their new positions to some degree (see Section 4).

4. Discussion

In this work we studied the interaction between the pro-apoptotic protein caspase-3 and its natural inhibitor, the anti-apoptotic protein calbindin-D28K. Calbindin-D28K is one of many Ca^{2+}-binding proteins within a cell, but the only one that is seen to directly bind caspase-3 [9]. The implications of this interaction are of significant interest in the areas of general apoptosis [21,22], cancer [21,23], neurodegenerative disease [22,24,25] and diabetes [26–28].

Previous NMR studies show that calbindin-D28K appears to undergo a conformational change between its apo- and fully Ca^{2+}-loaded states, while CD studies show it maintains the same level of α-helical content. This suggests that the helices shift conformation but neither extend/unravel as more Ca^{2+} binds. Subsequent ITC studies showed that apo-calbindin-D28K does not bind caspase-3. This implies that apo-calbindin-D28K does not contain the minimum structural motif required for caspase-3 recognition. The addition of a single Ca^{2+} to calbindin-D28K appears to provide enough of a structural change that this minimum recognition motif appears, since $1Ca^{2+}$-loaded calbindin-D28K binds to caspase-3. This interaction occurs predominantly according to a two-site binding model. As calbindin-D28K becomes more Ca^{2+}-loaded we observe that the protein continues to interact with caspase-3, though the interaction moves towards a one-site binding model. When calbindin-D28K becomes fully Ca^{2+}-loaded it interacts with caspase-3 primarily in a one-site binding mode. The evolution of a 'two-state-to-one-state' binding model lends weight to previous NMR and mass spectrometric studies on calbindin-D28K which suggest that the protein passes from an ordered apo-state through flexible states at intermediate levels of Ca^{2+}-binding, to a different ordered state when fully Ca^{2+}-loaded [10]. In the intermediate Ca^{2+}-loaded states the protein appears to possess sufficient flexibility to contact caspase-3 in a two-site fashion. This means that D28K contacts caspase-3 in two independent, non-symmetric locations. It is likely that these two contact regions are located quite close to one another.

As the protein becomes more ordered when fully Ca^{2+}-loaded, the concomitant loss of flexibility assures a single binding mode. Most importantly, these studies demonstrate that the interaction between calbindin-D28K and caspase-3 *is dependent* on the level of Ca^{2+} bound to calbindin-D28K. NMR NH-HSQC spectra of apo-calbindin-D28K and fully Ca^{2+}-loaded calbindin-D28K are shown in Supplementary Fig. 4 to illustrate this conformational change.

Molecular modeling/docking studies were carried out in order to provide the first detailed insights into the calbindin-D28K/caspase-3 interaction and to suggest a mechanism by which calbindin-D28K may inhibit caspase-3 function. Caspase-3 displays tremendous preference for the peptide sequence DEVD, enabling a 20,000-fold preference for aspartic acid over glutamic acid [4]. Such selectivity is due to very specific active site characteristics, which are in large part driven by the active site loops. Within these loops there are several stabilizing hydrogen bond and charge-charge interactions that are necessary to correctly align the active site. If anything perturbs this precise arrangement, then cleavage cannot occur and caspase-3 function is impeded.

Our studies predicted three possible binding models for the calbindin-D28K/caspase-3 interaction, with one of the binding modes containing 70% of the solved structures (cluster-1) (Supplementary Fig. 3A). In the cluster-1 model, calbindin-D28K's primary areas of contact with caspase-3 reside in EF-hands 1 and 2, with residues 33–50 (GKELQNLIQELLQARKK) occupying the cleft between loops 1 and 4 of caspase-3. No residues from calbindin-D28K were predicted to directly interfere with caspase-3's catalytic residues. However, calbindin-D28K does take up position such that access to the catalytic cleft is hampered. Certainly this would affect the ability of caspase-3 to perform its enzymatic function.

This model is consistent with the structures solved for other complexes between caspase-3 and: (i) XIAP_BIR2 (PDB:1I30) and (ii) DARPIN-3.4 (PDB:2XZD) (Fig. 4A and B, respectively). Although, slightly different, in both these cases XIAP_BIR2 and DARPIN-3.4 are positioned such that the caspase-3 active site is occluded. The two interactions are different however. In the caspase-3/XIAP_BIR2 complex, direct contacts between XIAP_BIR2 and the caspase-3 catalytic site are seen (contacts ~3 Å). As a note, in the caspase-3/XIAP_BIR2 complex, the caspase-3 catalytic residue Cys 163 was mutated to alanine. Conversely, the casapse-3/DARPIN-3.4 complex shows that no DARPIN residues are closer than 5 Å to the caspase-3 catalytic residues. This latter binding event is more similar to the caspase-3/calbindin-D28K complex modeled here (Fig. 4C). For the modeled caspase-3/calbindin-D28K complex (cluster-1) there are also no direct contacts seen between calbindin-D28K and the catalytic residues in caspase-3. The calbindin-D28K residue Asn 38 is the closest residue to the caspase-3 catalytic residues His 121 and Cys 163, at ~6 Å (Cα–Cα).

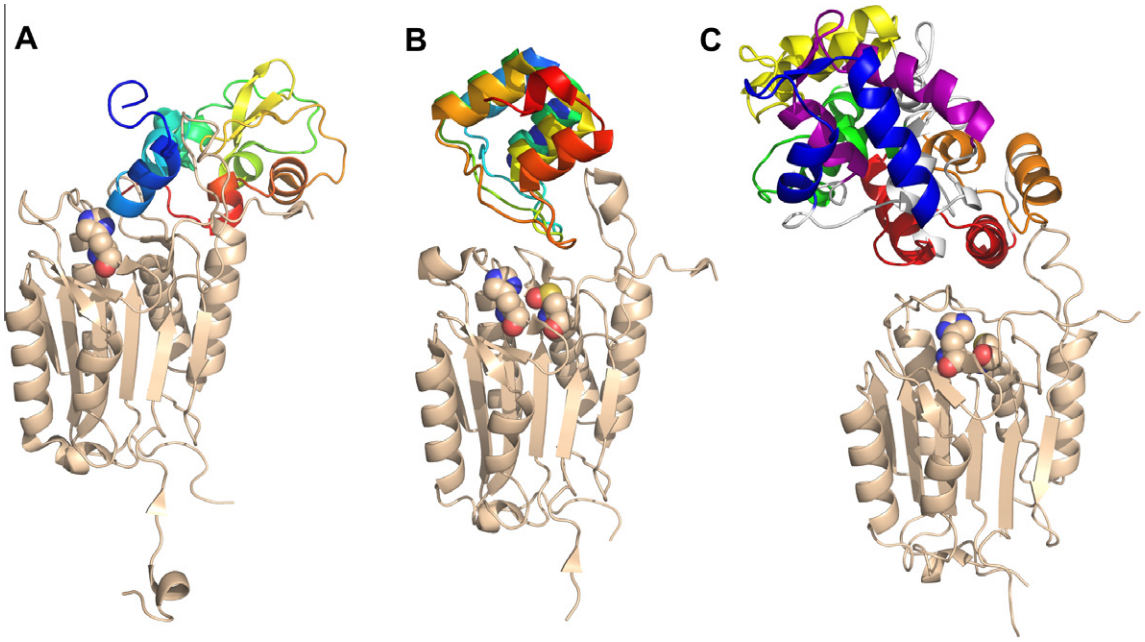

Fig. 4. Known caspase-3/protein (non-peptide) interactions. (A) Crystal structure of the complex between XIAP_BIR2 and C163A caspase-3. (B) Crystal structure of the complex between DARPIN-3.4 and caspase-3. (C) Lowest energy AMBER refined complex between calbindin-D28K and caspase-3. Caspase-3 is colored beige; catalytic residues are shown as spheres with hydrogens removed except panel (A). Calbindin-D28K has identical coloring schemes as in Fig. 2.

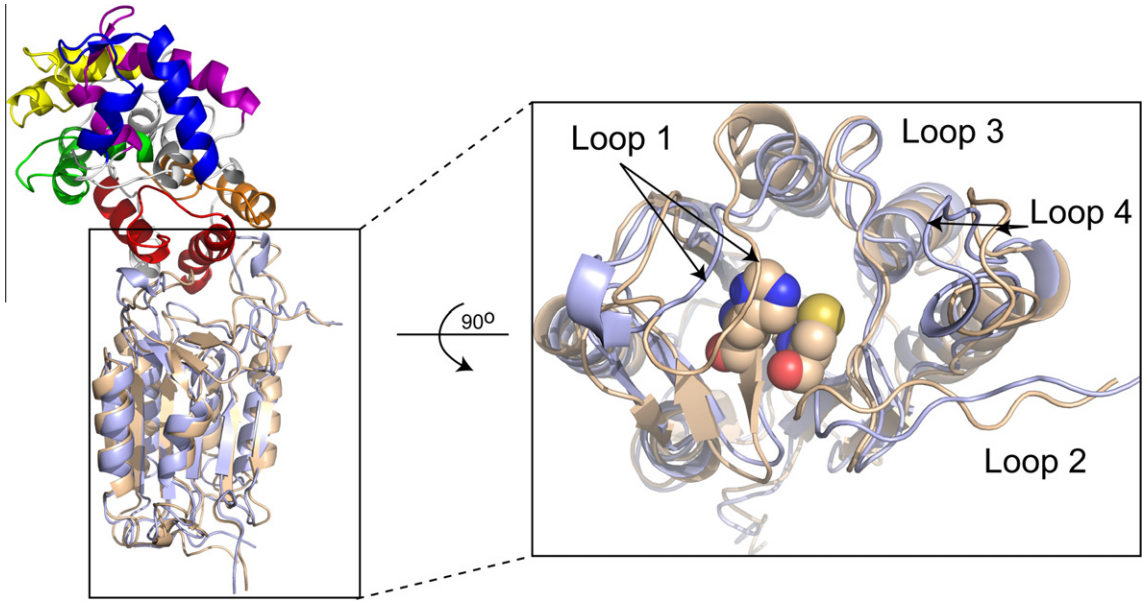

Fig. 5. Alternate loop conformations of caspase-3. The lowest energy AMBER refined complex between calbindin-D28K and caspase-3 overlaid with caspase-3 prior to docking. Docked caspase-3 is colored in beige while calbindin-D28K is colored identical to Fig. 2. Caspase-3 prior to docking (PDB:1CP3) is colored light blue. The image is rotated 90 degrees to clearly show the conformational changes that the labeled loops undergo upon binding calbindin-D28K. Caspase-3 catalytic residues are shown as spheres with hydrogens removed.

In addition to calbindin-D28K simply occupying a position that restricts substrate entry to caspase-3's catalytic cleft, our modeling studies suggest another potential contribution to caspase-3 inhibition. Previously the active site loops in caspase-3 have been shown to be critical to its activation, possibly through dynamic motions as seen in molecular dynamic simulations [20,29]. In the molecular modeling performed here, caspase-3 principally uses the active site loops to interact with several regions of calbindin-D28K, primarily EF-hands 1 and 2 (Figs. 4 and 5) [20]. Comparing the positions of the loops in caspase-3 before and after the docking (cluster-1), it is seen that loops 2 and 3 undergo only slight conformational rearrangement. However, significant conformational changes are seen for both loops 1 and 4 (Fig. 5). In the docked model of the caspase-3/calbindin-D28K complex the presence of the calbindin-D28K alters the position of loop 1 from caspase-3 such that it occludes the catalytic site. The functional ability of caspase-3 may well be impeded due to this limited access for substrates. Concomitantly, the hydrogen bonding networks of both loops are altered, likely affecting critical conformational requirements for function (see Supplementary Table 1).

Subsequent conformational sampling simulations were performed, with emphasis on loops 1 and 4 of caspase-3 in both its unbound state and when in complex with calbindin-D28K (Fig. 6). Comparing loops 1 and 4 before and after calbindin-D28K binding shows that both exhibit reduced motional tendency in the bound state. The largest difference is for loop 1 where the reduction in conformational space being sampled is 22%. For loop 4 the reduction in conformational space being sampled is 15%. Not only does it appear that the position of loops 1 and 4 change upon calbindin-D28K binding, but also that both loops become more conformationally trapped. These reduced motions may also contribute to calbindin-D28K's ability to affect caspase-3 function.

Here we have demonstrated that the interaction between the anti-apoptotic protein calbindin-D28K and its target, the pro-apoptotic executioner protein caspase-3, is dependent on the amount of Ca^{2+} bound to calbindin-D28K. We also note that as the protein transitions from its ordered apo-structure to its ordered (but different structured) fully Ca^{2+}-loaded form, its helical content

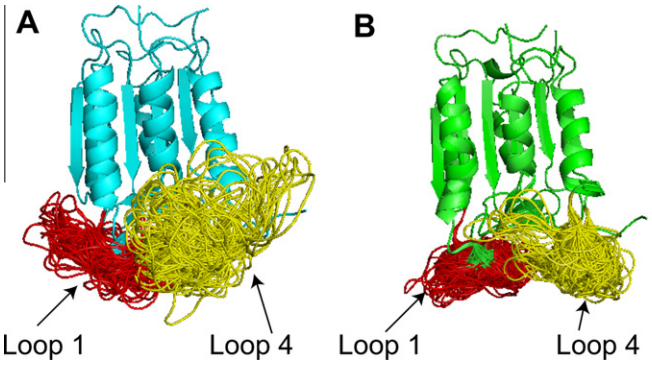

Fig. 6. Conformational sampling of caspase-3 loops 1 and 4. (A) Unbound caspase-3 (blue) with the calculated conformational space being sampled by loop 1 (red) and loop 4 (yellow). (B) Caspase-3 (green) when bound to calbindin-D28K with the calculated conformational space being sampled by loop 1 (red) and loop 4 (yellow). Note the reduction in sampled space by both loops in (B).

remains constant. Molecular modeling/docking studies using the high-resolution structures of caspase-3 and calbindin-D28K suggest that calbindin-D28K does not directly interact with the caspase-3 catalytic residues, supporting previous biochemical studies [9]. We propose a model of calbindin-D28K occupying a position that blocks the catalytic site on caspase-3. The concomitant shifting and reduction in motion of loop 1 (especially) and loop 4 in casapse-3 upon binding may also obstruct substrate access to the catalytic site and disrupt the optimum bonding network within the active site loops. These changes may adversely affect the apoptotic function of caspase-3. As far as we are aware this is the first model to describe a possible mechanism of action for the ability of calbindin-D28K to deactivate caspase-3. Finally, it is worth noting that in mature caspase-8, the position of loop 1 is such that the active site is available and ensures that catalytic activity can proceed. However, the NMR structure of inactive procaspase-8 shows that loop 1 adopts a position that occludes the active site [30]. This is a similar situation to that described here, supporting our model.

Here, loop 1 from caspase-3 is removed from the active site allowing proteolytic cleavage to occur unhindered. Loop 1 can be moved to obstruct the active site by the interaction with calbindin-D28K. It will be interesting to see if this proposed mechanism becomes a more general theme contributing to caspase inhibition.

Acknowledgements

The authors thank Dr. A.C. Clark (NCSU) for helpful discussions and for the caspase-3 construct and Dr. Rajiv Kumar (Mayo Clinic) for the calbindin-D28K construct. This work is supported by the V Foundation for Cancer Research.

Appendix A. Supplementary data

Supplementary data associated with this article can be found, in the online version, at http://dx.doi.org/10.1016/j.febslet.2012.08.032.

References

[1] Kerr, J.F., Wyllie, A.H. and Currie, A.R. (1972) Apoptosis: a basic biological phenomenon with wide-ranging implications in tissue kinetics. Br. J. Cancer 26, 239–257.
[2] Ashkenazi, A. (2002) Targeting death and decoy receptors of the tumour-necrosis factor superfamily. Nat. Rev. Cancer 2, 420–430.
[3] Martin, S.J. et al. (1996) The cytotoxic cell protease granzyme B initiates apoptosis in a cell-free system by proteolytic processing and activation of the ICE/CED-3 family protease, CPP32, via a novel two-step mechanism. EMBO J. 15, 2407–2416.
[4] Stennicke, H.R., Renatus, M., Meldal, M. and Salvesen, G.S. (2000) Internally quenched fluorescent peptide substrates disclose the subsite preferences of human caspases 1, 3, 6, 7 and 8. Biochem. J. 350 (Pt 2), 563–568.
[5] Lavrik, I.N., Golks, A. and Krammer, P.H. (2005) Caspases: pharmacological manipulation of cell death. J. Clin. Invest. 115, 2665–2672.
[6] Samuelsson, B. and Fondazione Giovanni Lorenzini (2001) Advances in Prostaglandin and Leukotriene Research: Basic Science and New Clinical Applications, Kluwer Academic Publishers; Fondazione Giovanni Lorenzini; Giovanni Lorenzini Medical Foundation, Dordrecht Boston; Milan, Italy; Houston, TX, USA.
[7] Liu, Y. et al. (2004) Prevention of glucocorticoid-induced apoptosis in osteocytes and osteoblasts by calbindin-D28K. J. Bone Miner. Res. 19, 479–490.
[8] Iacopino, A., Christakos, S., German, D., Sonsalla, P.K. and Altar, C.A. (1992) Calbindin-D28K-containing neurons in animal models of neurodegeneration: possible protection from excitotoxicity. Brain Res. Mol. Brain Res. 13, 251–261.
[9] Bellido, T., Huening, M., Raval-Pandya, M., Manolagas, S.C. and Christakos, S. (2000) Calbindin-D28K is expressed in osteoblastic cells and suppresses their apoptosis by inhibiting caspase-3 activity. J. Biol. Chem. 275, 26328–26332.
[10] Venters, R.A. et al. (2003) The effects of Ca(2+) binding on the conformation of calbindin D(28K): a nuclear magnetic resonance and microelectrospray mass spectrometry study. Anal. Biochem. 317, 59–66.
[11] Kordys, D.R., Bobay, B.G., Thompson, R.J., Venters, R.A. and Cavanagh, J. (2007) Peptide binding proclivities of calcium loaded calbindin-D28K. FEBS Lett. 581, 4778–4782.
[12] Kojetin, D.J., Venters, R.A., Kordys, D.R., Thompson, R.J., Kumar, R. and Cavanagh, J. (2006) Structure, binding interface and hydrophobic transitions of Ca2+-loaded calbindin-D(28K). Nat. Struct. Mol. Biol. 13, 641–647.
[13] J.B. Denault, G.S. Salvesen, Expression, purification, and characterization of caspases, Curr. Protoc. Protein Sci. 21 (2003) 13.
[14] Mittl, P.R., Di Marco, S., Krebs, J.F., Bai, X., Karanewsky, D.S., Priestle, J.P., Tomaselli, K.J. and Grutter, M.G. (1997) Structure of recombinant human CPP32 in complex with the tetrapeptide acetyl-Asp-Val-Ala-Asp fluoromethyl ketone. J. Biol. Chem. 272, 6539–6547.
[15] Dominguez, C., Boelens, R. and Bonvin, A.M. (2003) HADDOCK: a protein-protein docking approach based on biochemical or biophysical information. J. Am. Chem. Soc. 125, 1731–1737.
[16] D.A. Case, T.A. Darden, T.E. Cheatham III, C.L. Simmerling, J. Wang, R.E. Duke, R. Luo, R.C. Walker, W. Zhang, K.M. Merz, B. Roberts, B. Wang, S. Hayik, A. Roitberg, G. Seabra, I. Kolossvai, K.F. Wong, F. Paesani, J. Vanicek, J. Liu, X. Wu, S.R. Brozell, T. Steinbrecher, H. Gohlke, Q. Cai, X. Ye, J. Wang, M.-J. Hsieh, G. Cui, D.R. Roe, D.H. Mathews, M.G. Seetin, C. Sagui, V. Babin, T. Luchko, S. Gusarov, A. Kovalenko, P.A. Kollman, Amber, 11 ed., University of California, San Francisco, 2010.
[17] Hooft, R.W., Vriend, G., Sander, C. and Abola, E.E. (1996) Errors in protein structures. Nature 381, 272.
[18] Laskowski, R.A., Rullmannn, J.A., MacArthur, M.W., Kaptein, R. and Thornton, J.M. (1996) AQUA and PROCHECK-NMR: programs for checking the quality of protein structures solved by NMR. J. Biomol. NMR 8, 477–486.
[19] Seeliger, D., Haas, J. and de Groot, B.L. (2007) Geometry-based sampling of conformational transitions in proteins. Structure 15, 1482–1492.
[20] Feeney, B., Pop, C., Swartz, P., Mattos, C. and Clark, A.C. (2006) Role of loop bundle hydrogen bonds in the maturation and activity of (Pro)caspase-3. Biochemistry 45, 13249–13263.
[21] Jung, E.M., Choi, K.C. and Jeung, E.B. (2011) Expression of calbindin-D28K is inversely correlated with proapototic gene expression in hydrogen peroxide-induced cell death in endometrial cancer cells. Int. J. Oncol. 38, 1059–1066.
[22] Wu, C.K., Thal, L., Pizzo, D., Hansen, L., Masliah, E. and Geula, C. (2005) Apoptotic signals within the basal forebrain cholinergic neurons in Alzheimer's disease. Exp. Neurol. 195, 484–496.
[23] Tsukamoto, Y. et al. (2006) Expression of calbindin-D28K in sporadic nephroblastomas of the chicken. Avian Dis. 50, 127–130.
[24] Odero, G.L. et al. (2010) Evidence for the involvement of calbindin D28k in the presenilin 1 model of Alzheimer's disease. Neuroscience 169, 532–543.
[25] Sun, S., Li, F., Gao, X., Zhu, Y., Chen, J., Zhu, X., Yuan, H. and Gao, D. (2011) Calbindin-D28K inhibits apoptosis in dopaminergic neurons by activation of the PI3-kinase-Akt signaling pathway. Neuroscience 199, 359–367.
[26] Bazwinsky-Wutschke, I., Wolgast, S., Muhlbauer, E. and Peschke, E. (2010) Distribution patterns of calcium-binding proteins in pancreatic tissue of non-diabetic as well as type 2 diabetic rats and in rat insulinoma beta-cells (INS-1). Histochem. Cell Biol. 134, 115–127.
[27] Parkash, J., Chaudhry, M.A., Amer, A.S., Christakos, S. and Rhoten, W.B. (2002) Intracellular calcium ion response to glucose in beta-cells of calbindin-D28K nullmutant mice and in betaHC13 cells overexpressing calbindin-D28K. Endocrine 18, 221–229.
[28] Reddy, D., Pollock, A.S., Clark, S.A., Sooy, K., Vasavada, R.C., Stewart, A.F., Honeyman, T. and Christakos, S. (1997) Transfection and overexpression of the calcium binding protein calbindin-D28K results in a stimulatory effect on insulin synthesis in a rat beta cell line (RIN 1046–38). Proc. Natl. Acad. Sci. U S A 94, 1961–1966.
[29] Walters, J., Swartz, P., Mattos, C. and Clark, A.C. (2011) Thermodynamic, enzymatic and structural effects of removing a salt bridge at the base of loop 4 in (pro)caspase-3. Arch. Biochem. Biophys. 508, 31–38.
[30] Keller, N., Mares, J., Zerbe, O. and Grutter, M.G. (2009) Structural and biochemical studies on procaspase-8: new insights on initiator caspase activation. Structure 17, 438–448.